THE JOURNAL OF PHYSICAL CHEMISTRY A
A JOURNAL OF THE AMERICAN CHEMICAL SOCIETY

pubs.acs.org/JPCA Article

Ab Initio Molecular Dynamics Study on the Interlayer Bonding of Few-Layer Graphene under Pressures

Minghao Guo, Kun Ni,* and Yanwu Zhu*

Cite This: https://doi.org/10.1021/acs.jpca.5c01834 Read Online

ACCESS | Metrics & More | Article Recommendations | Supporting Information

ABSTRACT: Studying the formation of diamane through simulation is crucial for exploring the synthesis of ultrathin diamond films with excellent physical properties. However, dynamic studies of the phase transition from few-layer graphene to diamane under pressures using ab initio molecular dynamics (AIMD) and investigations on the corresponding evolution of the electronic structure have not yet been reported. In this study, we combined AIMD with static electronic calculations to explore the geometric and electronic structure evolution of bilayer graphene under different pressure-transmitting media (PTM). It is found that the pressure required for surface functionalization of bilayer graphene decreases in the order of halogens, hydrogen, hydrogen halides, and hydroxyl-containing systems, attributed to their different affinity for charge transfer to graphene. Additionally, as the number of graphene layers increases, the surface functionalization becomes easier under most PTM, especially in hydrogen-, hydrogen halide-, and hydroxyl-containing systems. Our research provides valuable insight into a deeper theoretical understanding of the interlayer bonding mechanism, offering potential for the experimental fabrication of diamane.

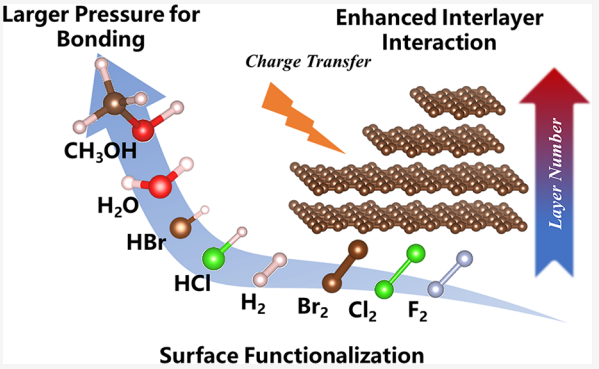

1. INTRODUCTION

A two-dimensional diamond with sp^3 hybridization between layers is called diamane.[1] Since the structure of diamane was proposed,[2] it has been considered valuable for high-power-density electronic devices under extreme conditions,[3] due to its excellent mechanical properties,[4,5] wide bandgap,[6] and high carrier mobility.[6] To explore the experimental synthesis, Gao et al. induced a reversible transformation from a bilayer epitaxial graphene film grown on SiC(0001) to a diamond-like structure via nanoindentation at room temperature, demonstrating the comparable stiffness and hardness to that of diamond.[5] Li et al. achieved reversible hydrogenation of single-layer graphene (SLG) by applying an ionic gate voltage between 2.2 and −1 V in a hydrogen-ion electrolyte (HTFSI).[7] The obtained structures mentioned above could not be retained after the pressure or the electric field was released.[5,7] Combining the external force with chemical induction may be more favorable for obtaining a stable diamane structure.[1] Barboza et al. used an electric force microscope to apply pressure to bilayer and multilayer graphene films in water via a scanning probe microscopy tip.[8] They observed that, with increasing tip pressure, the charging injection from the tip to bilayer and multilayer graphene was significantly suppressed, which could be explained by the formation of diamondol and was consistent with density functional theory (DFT) calculations.[8] Bakharev et al. fluorinated Bernal-stacked (AB stacking) bilayer graphene grown by chemical vapor deposition on a single-crystal CuNi(111) in a XeF_2 vapor under a pressure of 50−60 Torr at 65 °C and observed the formation of interlayer carbon−carbon bonds in a single-layer fluorinated diamond-like structure via angle-resolved X-ray photoelectron spectroscopy.[9] Despite the efforts made, the detailed formation of diamane from graphene layers is still insufficiently understood.

On the other hand, theoretical simulations can be used to search for the possible diamane structures through chemical group functionalization[10] or heteroatom doping.[11] Ge et al. systematically investigated 30 different diamane structures modified by various functional groups (H, F, OH, Cl, NH_2).[10] They identified 12 stable configurations based on formation energy, phonon spectra, and kinetic methods and analyzed their potential applications. Antipina et al. studied different configurations by modifying SLG, bilayer graphene (BLG), and trilayer graphene (TLG) with various chemical groups by DFT simulations, suggesting a tendency that few-layer graphene prefers to form a diamane structure.[12] They also proposed that hydrogen and fluorine adsorption can generally

Received: March 19, 2025
Revised: May 28, 2025
Accepted: May 28, 2025

ACS Publications © XXXX American Chemical Society

lead to a chair-type diamane, while water and ammonia cause more complex configurations.[12] However, these results have primarily been derived from direct structural optimization, which demonstrates only the final stable diamane structures. Further investigation on the detailed structural evolution mechanism using a molecular dynamics approach could give a much better description of the phase transition, compared to static optimization. For example, Wang et al. employed density functional tight binding molecular dynamics simulations to study the hydrogenation process of hexa-peri-hexabenzocoronene (HBC) in hydrogen plasma at temperatures ranging from 1000 to 2000 K, pointing out the critical role of interlayer interactions in stabilizing hydrogenated molecules.[13] However, studies using ab initio molecular dynamics (AIMD) could be limited by its high cost, and the in-depth study of the dynamical transformation for the formation of diamane from few-layer graphene is still lacking. The detailed analysis of the electronic structure evolution during phase transformation has not been reported yet, which is crucial for understanding the origin of diamane formation.

In this study, we investigate the interlayer bonding (IB) of few-layer graphene under pressure by combining AIMD simulations and detailed electronic structure analysis. We found that the pressure required for surface functionalization (SF) increases with the adsorption of certain chemical groups, which is in the following order of halogens, hydrogen gas, hydrogen halides, and hydroxyl-containing systems. In addition, the pressure required for SF decreases with an increasing number of graphene layers in most pressure-transmitting media (PTM), especially in hydrogen and hydrogen-bonded networks. Further electronic structure analysis, including Bader charge and density of states (DOS) calculations, reveals that the critical transformation pressure from BLG to diamane decreases as the charge transfer affinity from the functional groups to graphene increases. Our study improves the understanding of the formation mechanism from BLG to diamane and paves the way for more efficient fabrication and bandgap modulation of diamane, with potential applications in carbon-based semiconductors.

2. SIMULATION METHOD

All calculations were performed using the DFT method, by the Vienna ab-initio simulation package (VASP).[14−16] The Perdew−Burke−Ernzerhof (PBE)[17] exchange-correlation functional with generalized gradient approximation (GGA)[18] was adopted. The long-range van der Waals interactions were described using the Grimme DFT-D3 method with zero damping.[19] The basis set cutoff energy was 400 eV. The Brillouin zone was sampled with a 3 × 3 × 1 gamma-centered K-points grid for structural optimization. The projected density of states was calculated in two steps: (1) using a 10 × 10 × 1 gamma-centered K-points grid to calculate the charge distribution; (2) reading the charge distribution for the initial guess and performing a self-consistent field (SCF) calculation with a much denser gamma-centered K-points mesh of 25 × 25 × 1. The SCF calculation was performed with an energy convergence criterion of 10^{-4} eV. The geometry optimization force tolerance was 0.05 eV $Å^{-1}$.

The simulation cell has a lattice of 5.34 × 5.34 × 30 Å for a BLG model with various PTM (F_2, Cl_2, Br_2, H_2, HCl, HBr, H_2O, and CH_3OH) in the vacuum. The quasistatic compression process is shown in Figure 1, which consists of two stages. In the first stage, the lattice length along the OC direction was reduced step by step with a step size of 0.5 Å until the OC length reached the critical length ($OC_{critical}$) for the SF, and structural optimization was done after each step. In the second stage, the OC length was reduced by 0.1 Å in each step, starting from a distance of 1−2 Å longer than that of $OC_{critical}$, and an AIMD simulation with the canonical ensemble (NVT) at 300 K was performed during each compression step until the formation of diamane was observed.

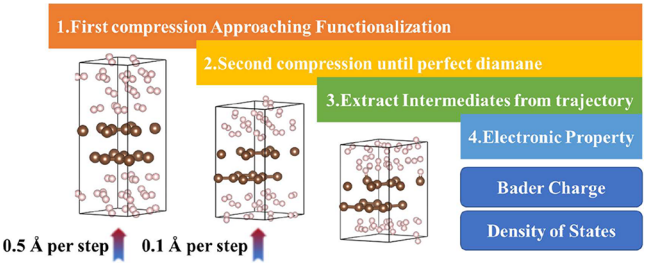

Figure 1. Schematic diagram of the structural transformation method used in PTM, along with the corresponding electronic structure evolution during the process.

The enthalpy change for the dissociation of a PTM molecule followed by adsorption on graphene was calculated using eq 1:

$$E_{dis} = E_{SF\text{-}G} + E_{res} - E_G - E_{Mol} \quad (1)$$

where $E_{SF\text{-}G}$ is the energy of graphene under SF conditions, E_{res} is the energy of the residual part of the molecules excluding functional groups, E_G is the energy of graphene, and E_{Mol} is the energy of PTM molecules before SF. The structure of PTM molecules and the structure used for calculating E_{res} were placed in a simulation cell with a lattice of 10 × 10 × 10 Å, and the Brillouin zone was sampled with a 1 × 1 × 1 gamma-centered K-points grid.

The average number of electrons lost from C atoms during the adsorption of graphene onto different PTM (F_2, Cl_2, Br_2, H_2, HCl, HBr, H_2O, and CH_3OH) was calculated using eq 2:

$$N_{e\text{-}loss} = 4 - Q_{ave} \quad (2)$$

where Q_{ave} is the averaged Bader charge of all carbon atoms from the SF structure in the trajectory of the AIMD simulation.

3. RESULTS AND DISCUSSION

To simulate the compression of the BLG in PTM, as illustrated in Figure 1 (details are shown in the simulation method), a gradually increasing pressure is applied onto the BLG through PTM by reducing the length of the OC lattice, in combination with structural optimization or AIMD relaxation. Key intermediate structures are extracted from the AIMD simulation trajectory for further Bader charge and DOS calculations to explore the evolution of electronic structure. PTM, including F_2, Cl_2, Br_2, H_2, HCl, HBr, H_2O, and CH_3OH, are simulated across a range of pressure loadings from 0 to 112.96 GPa. The AIMD results can directly show phase transitions and IB processes (Movies S1−S16).

The phase transition process can be regarded as the collaboration of two distinct parts: SF and IB. As shown in Figure 2a, for BLG in media such as F_2, Cl_2, Br_2, H_2, HCl, and HBr, SF occurs before IB. However, in H_2O and CH_3OH, IB occurs before SF. Previous studies have shown that SF with functional groups, e.g., H, F, and OH, facilitates the formation of interlayer bonds,[20,21] but our results show that SF does not precede IB in all PTM. The pressure required for the phase

https://doi.org/10.1021/acs.jpca.5c01834
J. Phys. Chem. A XXXX, XXX, XXX−XXX

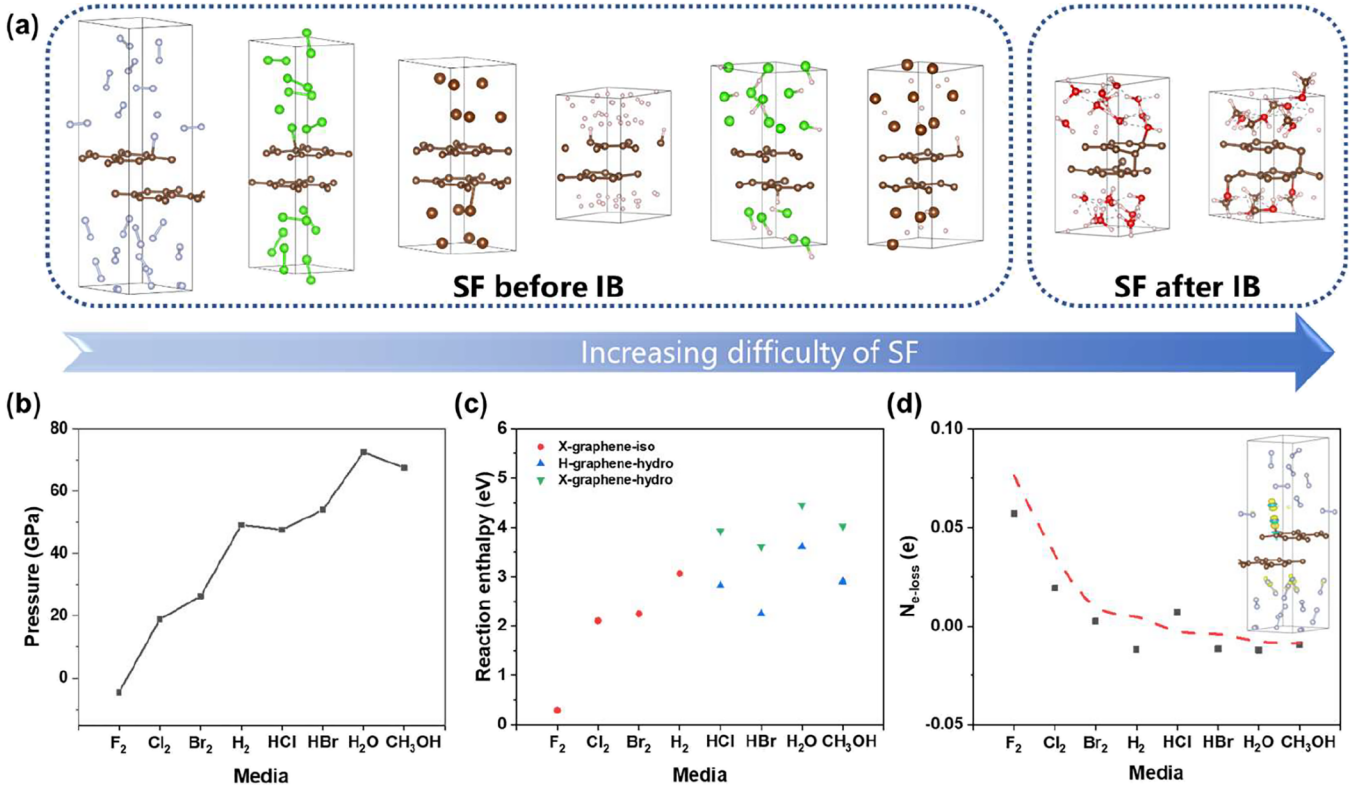

Figure 2. (a) Graphene SF structures in different PTM (F_2, Cl_2, Br_2, H_2, HCl, HBr, H_2O, and CH_3OH). (b) Ranking of different PTM by the pressure required for the SF. (c) E_{dis} in the isolated halogen molecule (X-graphene-iso, X represents the negative functional group) and hydrogen-bonded PTM (H_2, HCl, HBr, H_2O, and CH_3OH) (H-graphene-hydro and X-graphene-hydro, H represents the hydrogen atom and X represents the negative functional group). (d) $N_{e\text{-}loss}$ during the adsorption of graphene in different PTM (F_2, Cl_2, Br_2, H_2, HCl, HBr, H_2O, and CH_3OH), with the inset showing the differential charge density of graphene functionalized with F_2. The iso-surface value is 0.01 e^- $bohr^{-3}$.

transition corresponding to different PTM is ranked in Figure 2b, with halogens requiring the smallest pressure, followed by hydrogen, hydrogen halides, and finally hydroxyl-containing media like H_2O and CH_3OH, consistent with the out-of-plane structural deformation of BLG when the phase transition begins, as shown in Figure S1. The pressure needed for the functionalization of bilayer graphene by hydrogen atoms and hydroxyl groups is reported as 19.3 GPa by Varlamova et al.,[22] using a different method of evaluating pressure, compared to our approach. In addition, the limited size (0.53 nm) of our simulation cell may lead to a higher estimated phase transition pressure, caused by insufficiently released stress of graphene after SF. However, increasing the cell size to 1.07 nm did not give a significantly better description of the system, as shown in Figure S2, but it will reach the limitation of AIMD computation cost.

To give a deeper understanding of the preference for IB or SF, we calculated the enthalpy change for the dissociation of the PTM molecule followed by the adsorption on graphene (E_{dis}) (detailed information in simulation method), as shown in Figure 2c. From halogens, hydrogen, hydrogen halides to hydroxyl-containing media, E_{dis} maintains the same ranking as the pressure required for SF, as shown in Figure 2b and Table S1, consistent with the conclusion of Antipina et al.[12] The E_{dis} on the H-side is lower than on the X-side (X represents the negative functional group) in HCl and HBr, while the difference between the two adsorption sides for H_2O and CH_3OH is reduced. This is consistent with the results in Figure 2a, where graphene preferentially bonds to hydrogen atoms in HCl and HBr. Our results have shown that the adsorption affinity of PTM molecules with different orientations could be related to the difficulty of SF. In addition, E_{dis} for an isolated (-iso) PTM molecule and two hydrogen-bonded (-hydro) PTM molecules follows the same trend, except for H_2O molecules in Figure S3, indicating that hydrogen-bonding does not affect the adsorption affinity of the H-side or X-side of most of the PTM molecules mentioned above.

Furthermore, we calculated the average number of losing electrons in C atoms ($N_{e\text{-}loss}$) of graphene during SF (details are shown in eq 2 in the simulation method). The $N_{e\text{-}loss}$ of graphene during SF gradually decreases in the same order, as shown in Figure 2d, implying an influence from the charge transfer process, as indicated in the inset. DOS analysis also provides further understanding of the formation mechanism of chemical bonding. For those PTM without hydrogen bonds, as shown in Figure S4a−d, along the sequence of F_2, Cl_2, Br_2, and H_2, the energy overlap between the electron energy states provided by adsorption site and the functional group decreases, indicating a weaker bonding tendency between the graphene and the PTM molecules, in agreement with the pressure required for SF shown in Figure 2b. For those PTM with a hydrogen bond, as shown in Figure S5a−d, along the sequence of HCl, HBr, H_2O, and CH_3OH, the energy of the electron states of PTM decreases, resulting in the less overlap between the DOS of PTM and the DOS of adsorption site, leading to the weaker interaction between PTM molecules and graphene and higher functionalization pressure, in agreement with Figure 2b.

https://doi.org/10.1021/acs.jpca.5c01834
J. Phys. Chem. A XXXX, XXX, XXX−XXX

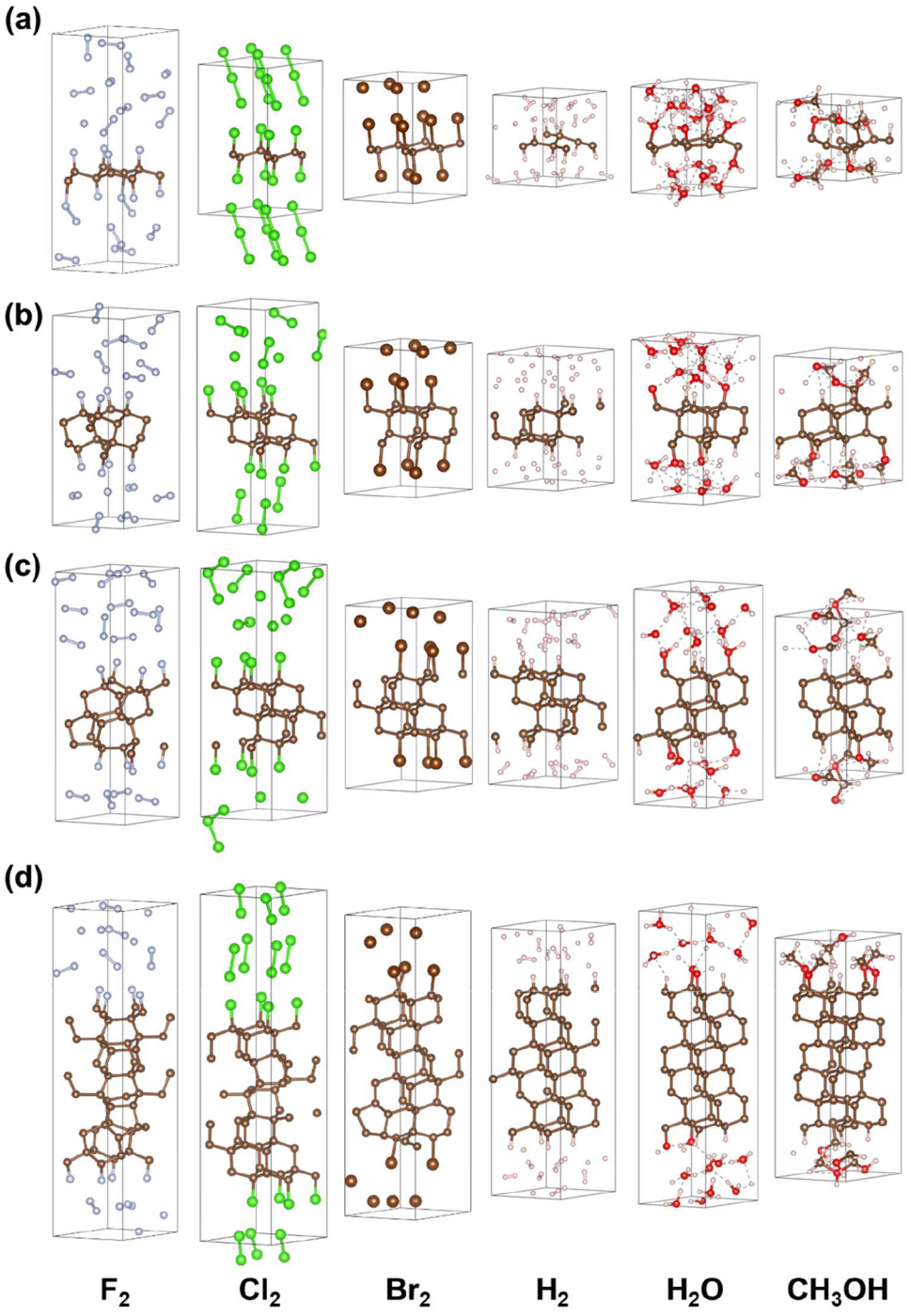

Figure 3. Final structures of (a) SLG, (b) BLG, (c) TLG, and (d) six-layer graphene (6LG) in different pressure-transmitting media (F_2, Cl_2, Br_2, H_2, H_2O, and CH_3OH).

The integrity of the formed diamane structure shows a dependency on the number of layers. As shown in Figures 3a and S6a,b, the structures formed from SLG with halogen atoms under sufficient pressure are relatively uniform, whereas those formed with hydrogen atoms or hydrogen-bonded systems are not easily achieved. Compared with halogens, the higher difficulty in initiating SF on graphene for H_2 and hydrogen-bonding PTM leads to an increased phase transition pressure. The difference in SF barriers across different sites on the graphene surface is subsequently reduced at higher pressure, making SF occur with less symmetric constraints, leading to the formation of disordered structures on SLG. This conclusion differs from that of BLG in Figure 3b, which consistently forms a uniform structure with all types of PTM under compression. For TLG, as shown in Figure 3c, fluorine atoms functionalize both sides of graphene, leading to an uncontrollable final structure that is difficult to uniformly form, while for the rest of the PTM, TLG still transforms to uniform structures. As shown in Figure 3d, when the number of layers increases to six, it is difficult for halogen elements to form uniform structures, while the advantage of hydrogen gas and hydrogen-bonded media in forming uniform structures

https://doi.org/10.1021/acs.jpca.5c01834
J. Phys. Chem. A XXXX, XXX, XXX−XXX

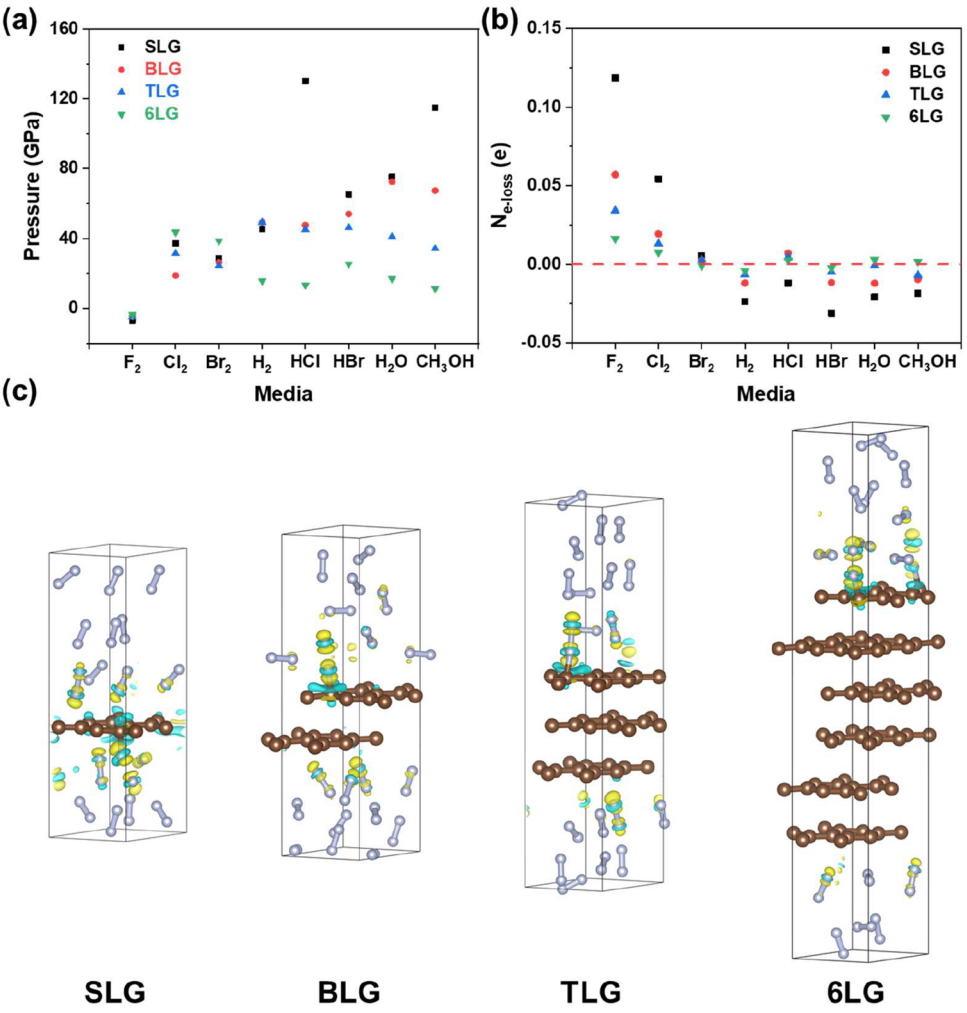

Figure 4. (a) Pressure required for SF of SLG, BLG, TLG, and 6LG in different PTM and (b) corresponding $N_{e\text{-loss}}$ during the adsorption of graphene in different PTM. (c) Differential charge densities of SLG, BLG, TLG, and 6LG functionalized in F_2. The iso-surface value is 0.005 e^- $bohr^{-3}$.

becomes evident. For halogen gas, e.g., F_2, as shown in Figure S7, phase transition propagates inward starting from the surface and leads to the formation of a disordered SF structure at the junction where the two transformation fronts converge. In H_2 and hydrogen-bonding media, as shown in Figure S8, multilayer graphene tends to form nuclei with the same orientation across adjacent layers, which then grow toward the surface, thereby facilitating the formation of a more uniform structure. Thus, SLG is more likely to form a uniform structure in the medium of halogen element monomers, while multilayer graphene intends to form a uniform structure in hydrogen, hydrogen halide, and hydroxyl-containing PTM.

The layer-dependent phase transition from BLG to diamane is further investigated by comparing the pressure required for SF of graphene and the corresponding charge transfer process. As shown in Figure 4a, for all the number of layers investigated, the pressure required for SF of graphene in F_2 approaches 0 GPa while the pressure required in bromine and chlorine gas gradually increases with the number of layers. However, H_2 and PTM containing hydrogen bonds show the opposite trend. The disagreements between our results and Erohin's reports could be explained by the asynchronous nucleation process observed in multilayer graphene during our AIMD simulation, as shown in Figure S8, which is different from Erohin's assumption of simultaneous phase transformation.[23] The change in the pressure for SF can also be explained by the $N_{e\text{-loss}}$ of graphene during SF, as shown in Figure 4b. The $N_{e\text{-loss}}$ of graphene in F_2, Cl_2, and Br_2 is greater than zero during SF, indicating that electrons are being withdrawn from graphene and the exclusion of P_z electron is weakened, lowering the pressure needed for SF. However, in H_2, HCl, HBr, H_2O, or CH_3OH, $N_{e\text{-loss}}$ of graphene is less than zero, indicating that electrons are being injected into graphene, which requires a significantly higher pressure to promote SF. As the number of layers increases, the number of charges extracted from graphene or injected into graphene by PTM during SF gradually decreases for F_2 (Figure 4c) and Cl_2, Br_2, H_2, HCl, HBr, H_2O or CH_3OH PTM (Figure S9a–d) due to more pronounced interlayer interaction, which is consistent to the decreased pressure for IB in hydrogen-bonded PTM for more graphene layers (Figure S10). The combination of weakened surface interaction and strengthened interlayer interaction results in a gradual reduction in the pressure required for SF corresponding to decreased charge injected into graphene in the H_2, HCl, HBr, H_2O, or CH_3OH systems. In addition, the increased pressure loading rate (2 Å/ps) results in a lower critical phase transformation pressure, compared to 0.5 and 0.1 Å/ps, as shown in Figures S11–S14

https://doi.org/10.1021/acs.jpca.5c01834
J. Phys. Chem. A XXXX, XXX, XXX−XXX

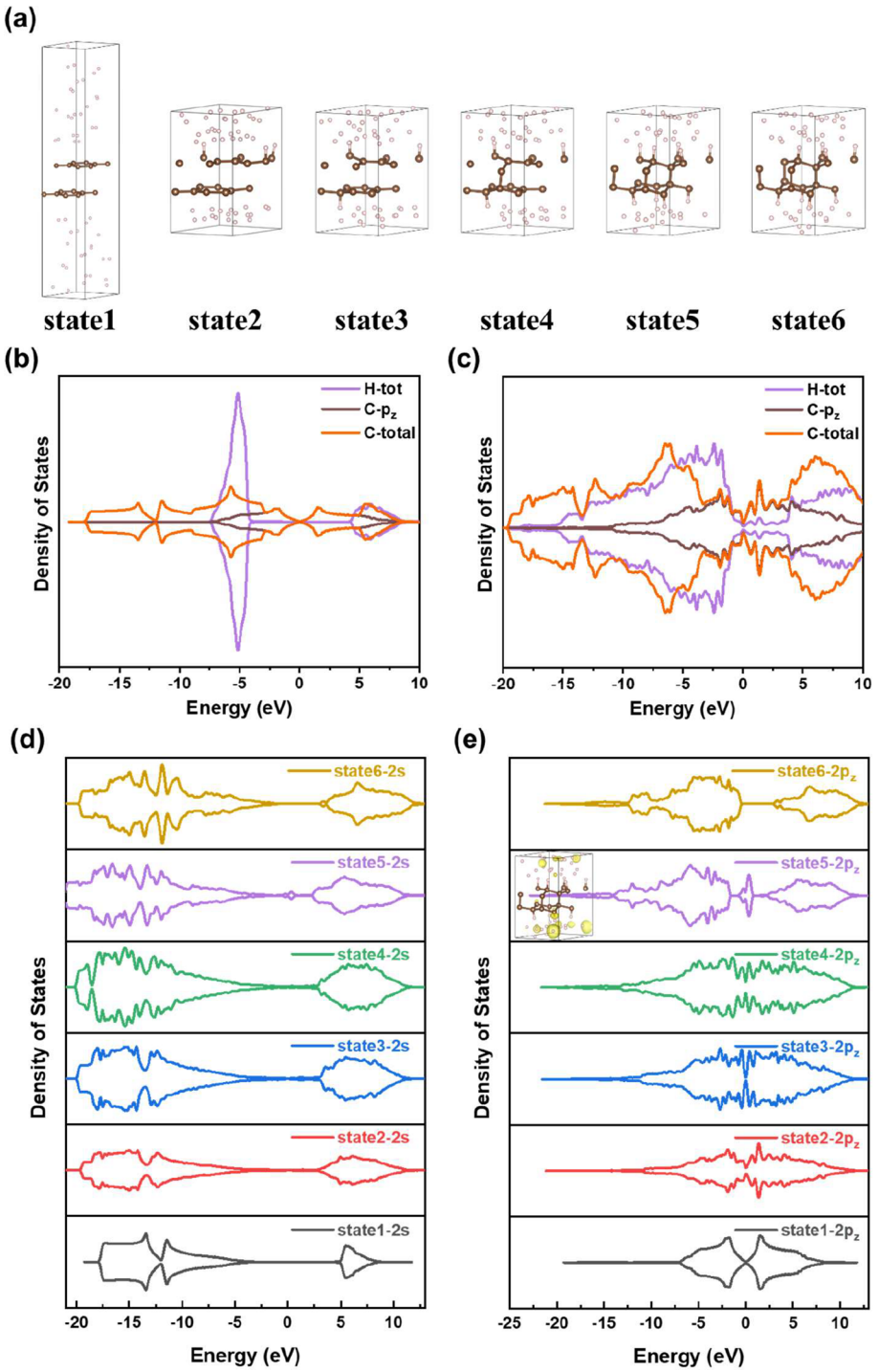

Figure 5. (a) Six states during compression of BLG in H_2 to form diamane and the corresponding projected density of states (PDOS) of graphene and hydrogen atoms for (b) state1 (adsorption) and (c) state2 (single-sided functionalization). PDOS of (d) 2s electrons and (e) p_z electrons in these states with the inset showing the partial charge distribution near the Fermi level for state 5. The iso-surface value is 0.01 e bohr^{-3}.

and Table S2, indicating that the shock-wave induced dynamic limitation facilitates the phase transition.

To elucidate the origins of SF and IB in BLG, we employed H_2 PTM as a model for comprehensive electronic structure analysis. As illustrated in Figure 5a, the structural evolution of compressed BLG in H_2 progresses through six distinct stages: adsorption, single-sided SF, double-sided SF, IB, oversaturated hydrogen SF, and structural repair. The corresponding PDOS for each state is presented in Figures 5b,c and S15a−d. The oversaturated SF in H_2 arises from hydrogen adsorption on adjacent carbon atoms during the initial SF on graphene, which is energetically favorable, as demonstrated in state 2 of Figure 5a. Figure 5b reveals that the PDOS of hydrogen gas adsorbed on graphene exhibits isolated, symmetric peaks, consistent with physical adsorption as reported in a previous study.[24] As the pressure increases along the out-of-plane direction, the PDOS of hydrogen gradually broadens and overlaps with the energy of p_z electrons of carbon, indicating the enhanced interactions between H_2 and graphene, as shown in Figure 5c.

https://doi.org/10.1021/acs.jpca.5c01834
J. Phys. Chem. A XXXX, XXX, XXX−XXX

The 2s electrons and p_z electrons in carbon atoms show significant changes during the pressure-induced SF and IB, as shown in Figure 5d, e. For 2s electrons, the occupied states move into deeper energy levels from states 1 to 5 as shown in Figure 5d, until a complete SF is finished, forming an oversaturated hydrogen adsorption structure. Then, the occupied states at low energy levels move to higher energy levels in state 6, with the desorption of hydrogen atoms to finish the structural repair, forming an ideal diamond. The energy of 2s electrons in carbon shows a similar trend, that is, moving toward a deeper energy level as more SF occurs. In addition, the partial charge density of graphene for the occupied states with the deepest energy level (from −17.9 to −21.2 eV) was calculated, showing a transition from in-plane C−C bonds to interlayer C−C bonds and C−H bonds from states 1 to 5, as shown in Figure S16a. Further calculations have shown that the 1s electron in hydrogen atoms and the 2s electron in carbon atoms exhibit synchronous behavior during SF, as depicted in Figure S16b,c.

As for the p_z electrons in carbon, the linear dispersion relation corresponding to the Dirac cone of graphene is disrupted with the pressure loading, and the PDOS near the Fermi surface gradually reveals multiple electronic states with close energy levels, as shown in states 1 to 3 in Figure 5e. Then, a defect state at the Fermi level is observed when the critical interlayer bonding is likely to happen, as shown in states 4 and 5 in Figure 5e. When the structural repair is finished, a large energy gap forms, as shown in state 6 in Figure 5e. The pressure-dependent bandgap could facilitate the in situ optical detection of the phase transition in experiments, as shown in Figure S17. The corresponding partial charge density for electrons near the Fermi level shows a transition from the π cloud in graphene to the σ bond in diamane, as shown in Figure S18. When more carbon atoms transform from sp^2 to sp^3 hybridization, the average energy of the p_z electrons in carbon gradually approaches the energy of the p_x and p_y electrons, as shown in Figure S19, leading to higher symmetry.

4. CONCLUSIONS

To provide a comprehensive understanding of the mechanism behind diamane formation, we have combined AIMD and static electronic calculations and revealed the correlation between the pressure required for SF of graphene and different PTMs, along with the corresponding theoretical origins. Further analysis shows that a stacking of more graphene layers promotes SF in most PTM, particularly in hydrogen- and hydrogen-bonded systems, which has also been supported from the perspective of electronic structure. We finalize the calculation by showing the consistency between changes in the electronic structure and structural transformation. Our work contributes to the study of diamane formation from a more comprehensive and fundamental perspective, which may be significant for the future advanced methods of controlling diamane synthesis.

■ ASSOCIATED CONTENT

Data Availability Statement

The structures reported in article is available at https://github.com/mhguo1997/data.

Supporting Information

The Supporting Information is available free of charge at https://pubs.acs.org/doi/10.1021/acs.jpca.5c01834.

More details including the simulation method and DFT calculations supporting our conclusions (PDF)

F_2 along the B-axis (AVI)

F_2 rotation 30° along the C-axis (AVI)

Cl_2 along the B-axis (AVI)

Cl_2 rotation 60° along the C-axis (AVI)

Br_2 along the B-axis (AVI)

Br_2 rotation 60° along the C-axis (AVI)

H_2 along the B-axis (AVI)

H_2 rotation 60° along the C-axis (AVI)

HCl along the B-axis (AVI)

HCl rotation 60° along the C-axis (AVI)

HBr along the B-axis (AVI)

HBr rotation 60° along the C-axis (AVI)

H_20 along the B-axis (AVI)

H_20 rotation 60° along the C-axis (AVI)

CH_3OH along the B-axis (AVI)

CH_3OH rotation 60° along the C-axis (AVI)

■ AUTHOR INFORMATION

Corresponding Authors

Kun Ni − *Department of Materials Science and Engineering, School of Chemistry and Materials Science, & Hefei National Research Center for Physical Sciences at the Microscale, & State Key Laboratory of Precision and Intelligent Chemistry, University of Science and Technology of China, Hefei, Anhui 230026, China*; Email: nikun@ustc.edu.cn

Yanwu Zhu − *Department of Materials Science and Engineering, School of Chemistry and Materials Science, & Hefei National Research Center for Physical Sciences at the Microscale, & State Key Laboratory of Precision and Intelligent Chemistry, University of Science and Technology of China, Hefei, Anhui 230026, China*; orcid.org/0000-0002-7505-1502; Email: zhuyanwu@ustc.edu.cn

Author

Minghao Guo − *Department of Materials Science and Engineering, School of Chemistry and Materials Science, & Hefei National Research Center for Physical Sciences at the Microscale, & State Key Laboratory of Precision and Intelligent Chemistry, University of Science and Technology of China, Hefei, Anhui 230026, China*

Complete contact information is available at: https://pubs.acs.org/10.1021/acs.jpca.5c01834

Author Contributions

M.G. conducted the simulations, analyzed the data and drafted the initial manuscript. K.N. contributed to the conceptualization of the study and provided revisions of the manuscript. Y.Z. supervised the research, provided revisions of the manuscript and secured the funding for this study.

Notes

The authors declare no competing financial interest.

■ ACKNOWLEDGMENTS

This work was supported by the Natural Science Foundation of China (Nos. 52273234, 52325202) and the Fundamental Research Funds for the Central Universities (WK2060000098, WK9990000170) and the open research fund of State Key Laboratory of Precision and Intelligent Chemistry (KY2490000300). The Supercomputing Center of USTC and the Hefei Advanced Computing Center is appreciated.

REFERENCES

(1) Liu, B.; Emmanuel, E.; Liang, T.; Wang, B. Advancements in theoretical and experimental investigations on diamane materials. *Nanoscale* **2023**, *15* (25), 10498−10512.

(2) Chernozatonskii, L. A.; Sorokin, P. B.; Kvashnin, A. G.; Kvashnin, D. G. Diamond-like C_2H nanolayer, diamane: Simulation of the structure and properties. *JETP Letters* **2009**, *90* (2), 134−138.

(3) Sorokin, P. B.; Yakobson, B. I. Two-Dimensional Diamond—Diamane: Current State and Further Prospects. *Nano Lett.* **2021**, *21* (13), 5475−5484.

(4) Cellini, F.; Lavini, F.; Cao, T.; de Heer, W.; Berger, C.; Bongiorno, A.; Riedo, E. Epitaxial two-layer graphene under pressure: Diamene stiffer than Diamond. *FlatChem.* **2018**, *10*, 8−13.

(5) Gao, Y.; Cao, T.; Cellini, F.; Berger, C.; de Heer, W. A.; Tosatti, E.; Riedo, E.; Bongiorno, A. Ultrahard carbon film from epitaxial two-layer graphene. *Nat. Nanotechnol.* **2018**, *13* (2), 133−138.

(6) Cheng, T.; Liu, Z.; Liu, Z. High elastic moduli, controllable bandgap and extraordinary carrier mobility in single-layer diamond. *Journal of Materials Chemistry C* **2020**, *8* (39), 13819−13826.

(7) Li, S.; Li, J.; Wang, Y.; Yu, C.; Li, Y.; Duan, W.; Wang, Y.; Zhang, J. Large transport gap modulation in graphene via electric-field-controlled reversible hydrogenation. *Nature Electronics* **2021**, *4* (4), 254−260.

(8) Barboza, A. P. M.; Guimaraes, M. H. D.; Massote, D. V. P.; Campos, L. C.; Barbosa Neto, N. M.; Cancado, L. G.; Lacerda, R. G.; Chacham, H.; Mazzoni, M. S. C.; Neves, B. R. A. Room-Temperature Compression-Induced Diamondization of Few-Layer Graphene. *Adv. Mater.* **2011**, *23* (27), 3014−3017.

(9) Bakharev, P. V.; Huang, M.; Saxena, M.; Lee, S. W.; Joo, S. H.; Park, S. O.; Dong, J.; Camacho-Mojica, D. C.; Jin, S.; Kwon, Y.; et al. Chemically induced transformation of chemical vapour deposition grown bilayer graphene into fluorinated single-layer diamond. *Nat. Nanotechnol.* **2020**, *15* (1), 59−66.

(10) Ge, L.; Liu, H.; Wang, J.; Huang, H.; Cui, Z.; Huang, Q.; Fu, Z.; Lu, Y. Properties of diamane anchored with different groups. *Phys. Chem. Chem. Phys.* **2021**, *23* (26), 14195−14204.

(11) Pakornchote, T.; Ektarawong, A.; Busayaporn, W.; Pinsook, U.; Bovornratanaraks, T. Roles of nitrogen substitution and surface reconstruction in stabilizing nonpassivated single-layer diamond. *Phys. Rev. B* **2020**, *102* (7), No. 075418.

(12) Antipina, L. Y.; Sorokin, P. B. Converting Chemically Functionalized Few-Layer Graphene to Diamond Films: A Computational Study. *J. Phys. Chem. C* **2015**, *119* (5), 2828−2836.

(13) Wang, Y.; Wang, Z.; Qiu, Z.; Zhang, X.; Chen, J.; Li, J.; Narita, A.; Müllen, K.; Palma, C.-A. Hydrogenation of Hexa-peri-hexabenzocoronene: An Entry to Nanographanes and Nanodiamonds. *ACS Nano* **2023**, *17* (19), 18832−18842.

(14) Kresse, G.; Furthmüller, J. Efficient iterative schemes for ab initio total-energy calculations using a plane-wave basis set. *Phys. Rev. B* **1996**, *54* (16), 11169−11186.

(15) Kresse, G.; Furthmüller, J. Efficiency of ab-initio total energy calculations for metals and semiconductors using a plane-wave basis set. *Comput. Mater. Sci.* **1996**, *6* (1), 15−50.

(16) Hafner, J. Ab-initio simulations of materials using VASP: Density-functional theory and beyond. *Journal of computational chemistry* **2008**, *29* (13), 2044−2078.

(17) Ernzerhof, M.; Scuseria, G. E. Assessment of the Perdew−Burke−Ernzerhof exchange-correlation functional. *J. Chem. Phys.* **1999**, *110* (11), 5029−5036.

(18) Perdew, J. P.; Burke, K.; Ernzerhof, M. Generalized Gradient Approximation Made Simple. *Phys. Rev. Lett.* **1996**, *77* (18), 3865−3868.

(19) Grimme, S.; Antony, J.; Ehrlich, S.; Krieg, H. A consistent and accurate ab initio parametrization of density functional dispersion correction (DFT-D) for the 94 elements H-Pu. *J. Chem. Phys.* **2010**, *132* (15), 154104.

(20) Paul, S.; Momeni, K. Mechanochemistry of Stable Diamane and Atomically Thin Diamond Films Synthesis from Bi- and Multilayer Graphene: A Computational Study. *J. Phys. Chem. C* **2019**, *123* (25), 15751−15760.

(21) Kvashnin, A. G.; Chernozatonskii, L. A.; Yakobson, B. I.; Sorokin, P. B. Phase Diagram of Quasi-Two-Dimensional Carbon, From Graphene to Diamond. *Nano Lett.* **2014**, *14* (2), 676−681.

(22) Varlamova, L. A.; Erohin, S. V.; Larionov, K. V.; Sorokin, P. B. Diamane Oxide. Two-Dimensional Film with Mixed Coverage and a Variety of Electronic Properties. *J. Phys. Chem. Lett.* **2022**, *13* (49), 11383−11390.

(23) Erohin, S. V.; Ruan, Q.; Sorokin, P. B.; Yakobson, B. I. Nano-Thermodynamics of Chemically Induced Graphene−Diamond Transformation. *Small* **2020**, *16* (47), No. 2004782.

(24) Liang, X.-Y.; Ding, N.; Ng, S.-P.; Wu, C.-M. L. Adsorption of gas molecules on Ga-doped graphene and effect of applied electric field: A DFT study. *Appl. Surf. Sci.* **2017**, *411*, 11−17.

https://doi.org/10.1021/acs.jpca.5c01834
J. Phys. Chem. A XXXX, XXX, XXX−XXX